Optical Flow Refinement using Reliable Flow Propagation

Tan Khoa Mai[1], Michèle Gouiffes[2] and Samia Bouchafa[1]
[1]*Université d'Evry Val d'Essonne, Evry, France*
[2]*LIMSI-CNRS, rue John Von Neumann, bât 508, Univ. Paris-Sud, Université Paris Saclay, Orsay, France*
{*tan-khoa.mai, samia.bouchafa*}*@ibisc.univ-evry.fr, michele.gouiffes@limsi.fr*

Keywords: Local Optical Flow, Reliability Measure, Propagation of Reliable Flow.

Abstract: This paper shows how to improve optical flow estimation by considering a neighborhood consensus strategy along with a reliable flow propagation method. Propagation takes advantages of reliability measures that are available from local low level image features. In this paper, we focus on color but our method could be easily generalized by considering also texture or gradient features. We investigate the conditions of estimating accurate optical flow and managing correctly flow discontinuities by proposing a variant of the well-known Kanade-Lucas-Tomasi (KLT) approach. Starting from this classical approach, a consensual flow is estimated locally while two additional criteria are proposed to evaluate its reliability. Propagation of reliable flow throughout the image is then performed using a specific distance criterion based on color and proximity. Experiments are conducted within the Middlebury database and show better results than classic KLT and even global methods like the well known Horn and Schunck or Black and Anandan approaches.

1 INTRODUCTION

Optical flow is one of the most important visual feature that is estimated from image sequences. It is considered as an essential visual cue not only for human vision but also in many applications that require segmentation, tracking or depth estimation.

Optical flow field, which must not be confused with 2D motion field, is the apparent motion that is caused by brightness variations. In order to estimate this field, most existing approaches start from the hypothesis that the brightness of a point is constant over time and then during its movement.

Since estimating optical flow is an ill-posed problem, last decades have given birth to a huge number of research works focusing on this topic. However, we can divide all the works into two main groups depending on the way they solve the estimation problem, whether it is done globally or locally in the image, *i.e* densely or sparsely. More precisely, global methods estimate velocity vectors of all of the pixels in the image at the same time by optimizing an energy function while local methods provide the optical flow of a limited number of specific points.

Horn and Schunck (Horn and Schunck, 1981) are pioneers of the global method. By adding a regularity term, the problem becomes well-posed and can be solved using optimization methods. The energy to be minimized is composed by two terms: a data term aiming at matching points of same brightness and a regularity term which imposes spatial smoothness of the velocity field. The energy function of Horn and Schunck often over-smooth the flows at the pixels located at the border of two or more moving areas. Up to now, the idea has attracted more than 2502 [1]researches, the objective of which was to improve the quality of the estimated motion by trying to solve the biggest limitations of Horn and Schunck, *i.e.* the discontinuities of motions. Many of them focused on modifying the cost function or suggesting different optimization methods (Black and Anandan, 1996; Wedel et al., 2009). The others exploit different features like color, gradient, texture (Wedel et al., 2009; Xu et al., 2010; Brox and Malik, 2011; Weinzaepfel et al., 2013; Kim et al., 2013). Some other researches perform first an object segmentation to help optical flow estimation(Sun et al., 2010; Chen et al., 2013; Yang and Li, 2015). All of these extensions try to find the flow by optimizing the modified energy function in a global way at the cost of a higher complexity.

On the other hand, local methods use a different hypothesis to overcome the ill-posed problem by taking into account only a small subset of pixels to optimize an energy function. The most popular lo-

[1]on http://www.sciencedirect.com

Mai T., Gouiffes M. and Bouchafa S.
Optical Flow Refinement using Reliable Flow Propagation.
DOI: 10.5220/0006131704510458
In *Proceedings of the 12th International Joint Conference on Computer Vision, Imaging and Computer Graphics Theory and Applications (VISIGRAPP 2017)*, pages 451-458
ISBN: 978-989-758-227-1

cal method comes from the work of Kanade-Lucas-Tomasi (Lucas and Kanade, 1981) where it is assumed that all N pixels in a fixed-size window have the same motion. This leads to an over-fitted problem where two unknown components of the motion vector are solved with N equations. The choice of the window size is critical. When too small, the aperture problem is not solved and the flow can not be estimated. When too large, it is likely to contain several values of motions, leading to inaccuracies.

Many research works try to overcome the difficulty of local methods like in (Black and Anandan, 1991; Bab-Hadiashar and Suter, 1998) where the classical quadratic error is replaced with a more robust function. In (Farneback, 2000; Black and Anandan, 1996), the authors use a parametric model of higher order by integrating the color information. A large number of researches focus on the analysis of the tensor structure. For example, (Nagel and Gehrke, 1998; Brox and Weickert, 2002; Middendorf and Nagel, 2001; Liu et al., 2003) investigate adaptive local neighborhoods while Nagel et al. (Middendorf and Nagel, 2001) analyze the tensor structure in order to segment the image into regions where flow are estimated. Finally, Liu et al. (Liu et al., 2003) analyze the tensor structure to find the best window size while Brox et al. (Brox and Weickert, 2002) propose to propagate nonlinear structure tensor in order to preserve the discontinuity by reducing the influence of the neighbors for which the gradient magnitude is high.

Because they produce a dense and regularized flow field, global methods provide better results than local methods in terms of precision. Somehow, by observing the results of both the classical methods Horn and Schunck and the KLT, the brightness invariance constraint is not always satisfied. The motion vectors for which the constraint is fulfilled are likely to be more accurate than the other motion vectors. The global optical flow can be improved by using the most reliable motion vectors to influence and correct the less reliable ones.

Starting from this basic idea, this paper proposes a novel approach to improve the optical flow by taking into account the violation or not of the brightness invariance constraint. The accuracy of the estimated flow vectors is evaluated by computing a *reliable score* that gives a kind of level of consensus in a neighborhood around each considered point. Even if our approach could be applied to any optical flow estimation method, we choose in this paper to illustrate the main principle by starting from the KLT method. After KLT estimation, a propagation process corrects the less reliable flows according to a distance measure based on color and proximity. Unlike all existing local methods that focus on the modification of the tensor structure and the estimation of the flow at the same time, our method provides a first estimation and correct it *a posteriori* depending on the reliability scores. Our paper is organized as follows. First, Section 2 investigates the relevance of the brightness constraint. Then, section 3 proposes a way to score the reliability of flows. Section 4 proposes a method to propagate the optical flow based on their reliable points. The numerical implementation is detailed in section 5 and experiments are given in 6, where our proposed method is compared to existing techniques. Finally, section 7 concludes the work and proposes new tracks.

2 OPTICAL FLOW AND BRIGHTNESS CONSTRAINT

The brightness constraint plays an important role in estimating flow vectors as it provides a basic motion constraint equation to be solved on each point. This section recalls its mathematical formulation and proposes a possibility for evaluating estimated flow reliability by exploiting this constraint.

Optical flow estimation relies on the assumption that the brightness value of a moving point p of coordinates $\mathbf{x} = [x,y]^\top$ is constant over time. Let us consider two successive images I_1 and I_2 in a video image sequence with the size of Q points and $\mathbf{u} = [u_x, u_y]^\top$ the motion vector associated to each point. Then $I_1(\mathbf{x}) = I_2(\mathbf{x}+\mathbf{u})$ with $I_1, I_2 : \mathbb{R}^2 \rightarrow \mathbb{R}^n$ where n is the number of image channels. In this paper, we choose to start from the KLT approach which is a local optical flow estimation method. This approach assumes that in a given neighborhood, flow vectors are similar and satisfy the brightness constraint equation. This assumption could be expressed as the minimization of energy function E:

$$min_u E = \sum_{p \in W} (I_1(\mathbf{x}) - I_2(\mathbf{x}+\mathbf{u}))^2 \qquad (1)$$

To solve $\mathbf{u}$ in (1), the image is generally linearized around vector $\mathbf{u}$, therefore (1) becomes:

$$\begin{aligned} I_2(\mathbf{x}+\mathbf{u}) &\approx I_2(\mathbf{x}) + \nabla I_2(\mathbf{x}).\mathbf{u} \\ I_2(\mathbf{x}) + \nabla I_2(\mathbf{x}).\mathbf{u} &= I_1(\mathbf{x}) \\ \nabla I_2(\mathbf{x}).\mathbf{u} &= I_1(\mathbf{x}) - I_2(\mathbf{x}) = -I_t \end{aligned}$$

So, the optimal solution $\mathbf{u}$ should lie on the line $\mathbf{a}^\top.\mathbf{u} + \mathbf{b} = 0$ where $\mathbf{a} = \nabla I_2(\mathbf{x}), \mathbf{b} = -\mathbf{I_t}(\mathbf{x})$. Since this is an ill-posed problem, the N points in the window W centered at the examined point allow to find

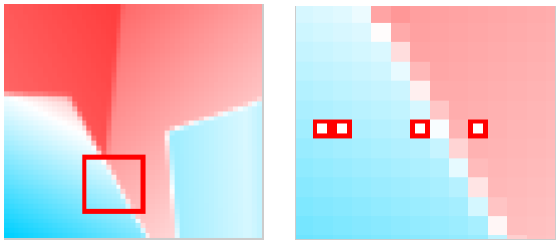

(a) (b)

Figure 1: The ground truth of sequence Venus of MiddleBury database. (a) ground truth with examined region in the red rectangle. (b) the zoomed examined region with 4 pixels to be investigated.

the solution. Indeed, the solution must satisfy:

$$min_u E = \sum_{p \in W} (\mathbf{u}.\nabla I_2 + I_t)^2$$

The coordinates of p are implicit for sake of clarity. Since the least-square error function is used to indicate the deviation of movement toward the constraint line, the optimal solution is found by simply deriving E according to u_x and u_y and finding the solution $\mathbf{u}$ that makes the partial derivatives of E equals zero. After development, this is equivalent to solve the following linear equation:

$$\mathbf{A}.\mathbf{u} = \mathbf{b} \text{ with:} \quad (2)$$

$$\mathbf{A} = \begin{bmatrix} \sum {I_2}^2{}_x & \sum I_{2x} I_{2y} \\ \sum I_{2x}.I_{2y} & \sum {I_2}^2{}_y \end{bmatrix} \text{ and } \mathbf{b} = \begin{bmatrix} \sum I_{2x} I_t \\ \sum I_{2y} I_t \end{bmatrix}$$

Ideally, the N points of the window all satisfy the brightness constraint and the resulting unique solution is likely to be correct. Of course, the solution can also come from the mixture of all the motion values present in the window. Hence, the estimated flow is likely to be incorrect or inaccurate. Let us take the example of the image sequence Venus from the MiddleBury database (Baker et al., 2010) the ground-truth of which is displayed in (Fig.1(a)). Fig.2 compares the estimated flow (black dot) with the true flow (red dot) and draws the line of brightness constraint of the mentioned points in (Fig.1(a)). Several situations can occur: the ideal case where the estimation is close to the ground-truth and close to constraint line (Fig.2 (a) and (b)), the case where even if the estimation is correct, the brightness constraint is not complied (Fig.2 (c)) and inversely a situation where the brightness constraint is fulfilled but the solution is inaccurate (Fig.2 (d)). Consequently, using this distance to the constraint line solely is not sufficient to evaluate the reliability of the estimated flow. A novel reliability criterion is defined in section 3.

3 OPTICAL FLOW RELIABILITY

This section proposes a new flow reliably score that allow us to quantify the reliability of the estimated flow. This section is devoted to the definition of this new criterion.

In the KLT method, the motion is estimated once for each point by taking into account the neighbors in a local window. Besides the classical corners-criterion of KLT, it is assumed in this work, that the motion computed at a point is reliable also when its value do not vary while shifting slightly the window around that point, as illustrated by Fig.3.

Thus, our supplementary criterion for reliability would be a factor to measure the convergence of estimated motions for each point by analyzing the distribution of its values. Fig.4 illustrates this assertion by showing the intensity profiles in two windows located either on a uniform region in terms of motion, or in a border between two regions of different motion. Fig.5 shows the distribution of estimated flows by shifting the window around four exact the same investigated points in (Fig.2). A point where all the values converge on the solution domain is more likely to be estimated correctly and *vice-versa*. A simple and intuitive way to evaluate the convergence is to compute the variance of these values. Calling S the set of solutions found by solving (2) with shifting windows (each solution is noted $\mathbf{s} \in S$) according to the explanation above for a specific point p with coordinates $\mathbf{x}$. The variance score for that point is defined as:

$$s_{var}(p) = \frac{1}{\sigma_S^2(p) + \varepsilon} \quad (3)$$

where ε is a small value used to avoid a zero at denominator. This score is normalized to become the following weight:

$$w_{var}(p) = \frac{s_{var}(p)}{\sum_{p \in Q} s_{var}(p)} \quad (4)$$

The second criterion would be the minimum eigenvalue of matrix $\mathbf{A}$ in (2) where p is in the center of window. This condition is designed to avoid homogeneous regions where the estimated motions have high w_{var} but are not reliable in terms of KLT condition.

$$\begin{bmatrix} \sum I_{2x}^2 & \sum I_{2x} I_{2y} \\ \sum I_{2x} I_{2y} & \sum I_{2y}^2 \end{bmatrix} \rightarrow eig(p) = \lambda_1, \lambda_1 < \lambda_2 \quad (5)$$

This value is normalized too:

$$w_{eig}(p) = \frac{eig(p)}{\sum_{p \in Q} eig(p)} \quad (6)$$

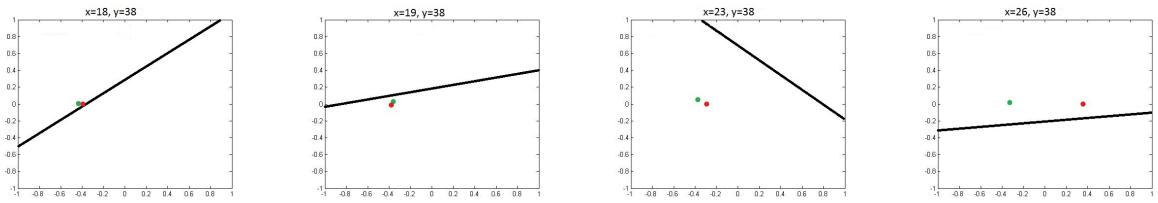

(a) (b) (c) (d)

Figure 2: Estimated flow (green dot) compared to its brightness constraint line and its ground truth (red dot). (a), (b): correct estimation of the optical flow and proximity with the constraint line. (c) : correct estimation but far from the constraint line; (d) incorrect estimation close to the constraint line.

Finally, the reliability weight is combined using the two weights defined above to satisfy the two mentioned conditions:

$$w_r = w_{var}.w_{eig} \tag{7}$$

The weight w_r is the final reliability score which is used in the propagation process explained hereafter.

4 PROPAGATION OF MOTION

This section details the propagation process that includes two main steps: determining a unique reliable flow on a given neighborhood and then propagating this flow under color and proximity criteria.

4.1 Estimation of the Optical Flow

Before propagating the flow, we have to estimate a unique flow for each point. From the set of solutions S that are available for each point p of coordinates $\mathbf{x}$, the solution is given by the weighted average of all flows. The weight is the inverse distance of the solution $\mathbf{s}$ to the constraint line of brightness $\nabla I_2(\mathbf{x}).\mathbf{s}+I_t=0$. This weighting process could be considered as a kind of consensus flow estimation in a neighborhood.

For each $\mathbf{s}$ in S, the weight is:

$$w_{err}(\mathbf{s}) = \frac{1}{|\nabla I_2(\mathbf{x}).\mathbf{s}+I_t|+\varepsilon} \tag{8}$$

and the estimated flow is then:

$$\mathbf{u}_e(p) = \frac{\sum_{\mathbf{s}\in S} w_{err}(\mathbf{s}).\mathbf{s}}{\sum_{\mathbf{s}\in S} w_{err}(\mathbf{s})} \tag{9}$$

$\mathbf{u}_e$ is the estimated flow of point p deducted from the set of solutions found by the algorithm. Some other strategies have been tested for the estimation $\mathbf{u}_e$. As shown further in section 6, they bring slightly different results.

With this value $\mathbf{u}_e$ and the reliable score w_r, the propagation can start.

4.2 Propagation of Reliable Flows

Object color presents generally a kind of global or at least partial uniformity. Moreover, the points that correspond to the same rigid object have similar motions. The idea is then to propagate high reliable flows onto pixels with low reliable ones under color and proximity (spatial distance) constraints. The propagation is performed using two steps:

1. Suggesting a new flow by using a consensus strategy.

The neighbor points in the window W centered in the examined point p will propose a new flow based on their influence to the examined point p. For each neighbor $q \neq p$ in W, an influence energy is calculated by:

$$e_{simi}(q,p) = e^{-\frac{d_{color}(q,p)}{\sigma_c} - \frac{d_s(q,p)}{\sigma_s}} \tag{10}$$

where d_{color} is the Euclidean RGB distance between p and its neighbor q and d_s is their spatial Euclidean distance.

The new flow is then computed by the weighted combination:

$$\widehat{\mathbf{u}_e}(p) = \frac{\sum_{q\in W, q\neq p} e_{simi}(q,p).\mathbf{u}_e(q)}{\sum_{q\in W, q\neq p} e_{simi}(q,p)} \tag{11}$$

Using the same principle, the new flow has its own reliable score that could be found using:

$$\widehat{w_r}(p) = \frac{\sum_{q\in W, q\neq p} e_{simi}(q,p).w_r(q)}{\sum_{q\in W, q\neq p} e_{simi}(q,p)} \tag{12}$$

2. Updating new flow and reliable score.

If the new reliability score of p is higher than the previous one, then its flow and reliability score are updated with the new values computed in (11) and (12). Hence, the propagation process is made using an iterative scheme where the reliability increases after each iteration. The procedure stops when all points get the same reliable score. Alternately, to accelerate the process, the procedure can stop when reliability or flow do not vary much.

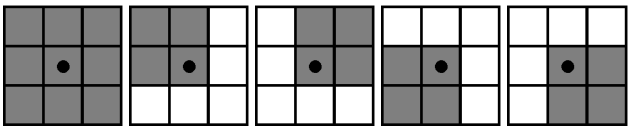

(a) (b) (c) (d) (e)

Figure 3: Illustration of shifting window around the examined point. (a): The classic KLT window where the point is always at the center.(b), (c), (d), (e): different positions of windows are applied around the point, each of them leads to a different motion value.

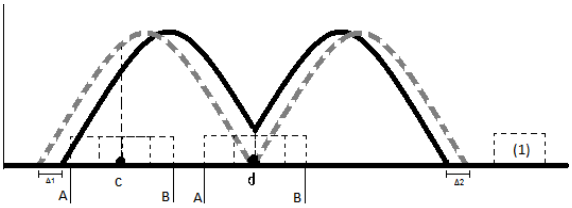

Figure 4: An 1-D illustration shows how the convergence of estimated flows can be a criterion for reliability. We suppose that the dotted gray line is a profile of intensity from the previous image I_1 while the black line represents the same profile I_2 after motion (Δ_1 and Δ_2 are two different movement directions). The abscissa axis represents the coordinates of the point and the ordinate axis represent its intensity. For each point "c", "d", the window (1) will slide in interval [A-B]. Intuitively, the window centered in "c" would collect motion values of good uniformity with a value close to Δ_1. On the contrary, the flows collected in the window centered in "d" are scattered between Δ_1 and Δ_2.

$$\begin{aligned} &\text{If } \widehat{w_r}(p) \geq w_r(p) \\ &\mathbf{u}_e(p) = \widehat{\mathbf{u}}_e(p) \\ &w_r(p) = \widehat{w_r}(p) \end{aligned} \tag{13}$$

Introducing the color similarity helps propagating the flow in an object-oriented way in which the points of close colors get more influence from each other than the others.

Table 1: Implementation of the proposed algorithm.

Input: Two color images I_1 and I_2
Output: Flow vector $\mathbf{u}$ from I_1 to I_2
• Convert color images to gray $I_1 \rightarrow G_1$, $I_2 \rightarrow G_2$
• Create L-levels pyramidal images for I_1, I_2 ,G_1, G_2
• Initialize $\mathbf{u}^L = \mathbf{u}_0 = 0$
For l = L to 1
  • Compute $\nabla I_1^l(\mathbf{x})$, $\nabla G_1^l(\mathbf{x})$
  For i = 1 to *Max_Warps*
    • Interpolate $I_2^l(\mathbf{x}+\mathbf{u}^l), G_2^l(\mathbf{x}+\mathbf{u}^l)$
    • Compute $\nabla I_2^l(\mathbf{x}+\mathbf{u}^l)$,$\nabla G_2^l(\mathbf{x}+\mathbf{u}^l)$
    • Compute I_t^l
    • Compute $\{\mathbf{s} \in S\}$ and determine the weight w_r according to (7) by using G_1,G_2 and their derivations
    • Estimated $\mathbf{u}_e$ from S following (9)
    • Modify $\mathbf{u}^l$ by using w_r and $I_2^l(\mathbf{x}+\mathbf{u}^l)$:
      For j=1 to *Max_Iteration*
        ► Calculate $\widehat{\mathbf{u}_e}$,$\widehat{w_r}$ for all of the pixels according to (11),(12)
        ► Collect the points whose $\widehat{w_r} > w_r$
        ► Modify their flow and reliable score according to (13)
      End
    • Apply median filter to $\mathbf{u}^l$
    • Prepare the next iteration $\mathbf{u}_{k-1} = \mathbf{u}^l$
  End
  • Propagate $\mathbf{u}^l$ to $\mathbf{u}^{l-1}$
  • $\mathbf{u}_k = \mathbf{u}^{l-1}$
End

5 IMPLEMENTATION

The numerical implementation of our method is given in Table.1. The scheme of pyramidal images and propagation of flows through pyramidal images are implemented in the similar way as in (Wedel et al., 2009). We focus here on the essential part of the proposed method.

6 EXPERIMENTS

Our new algorithm is applied to the Middlebury database in order to evaluate its performances for small movements. The experiments are conducted by using the pyramidal images and wrapping scheme to well estimate the flow. To find the flow using the local KLT method, we use a window size of 5×5 applied to the gray image. To propagate the flow using equation (13), color is considered as explained in previous sections and neighbors belong to a window of size 5×5. Moreover, $\sigma_c = 25$ and $\sigma_d = 2$.

Section 4.1 details the process used for estimating a consensual flow from a set of estimated flows by using a weighted average value. As mentioned before, in order to test the robustness of the consensual approach, three other possibilities have been tested: using a random flow among the solutions, using the closest solution from the constraint line and finally the

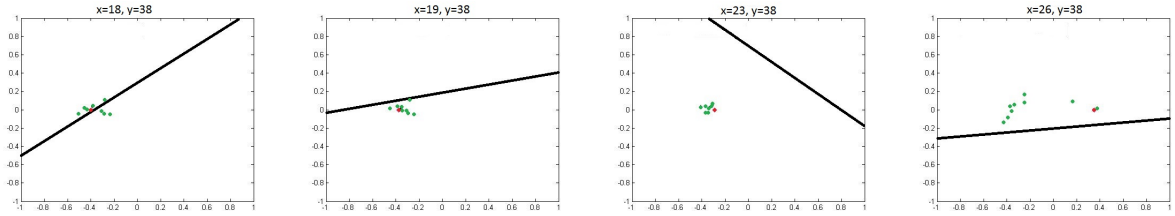

Figure 5: Distribution of estimated flows for each point after shifting the estimation windows. We create a cloud of solution S at each point.

original flow proposed in the KLT method. Table.2 and Table.3 show the error measures AAE[2] and EPE[3] after the propagation (Baker et al., 2010) for each approach and confirms the relevance of the weighted average.

Table 2: Accuracy of different strategies to choose a unique flow from the set of candidates of two sequences Venus and RubberWhale.

Database	Venus		RubberWhale	
Approach	AAE	EPE	AAE	EPE
Average weight	4.054	0.261	3.558	0.114
Random	4.096	0.273	3.656	0.116
Closest	4.219	0.277	3.606	0.116
KLT	4.167	0.267	3.671	0.117

Table 3: Accuracy of different strategies to choose a unique flow from the set of candidates of two sequences Grove2 and Urban2.

Database	Grove2		Urban2	
Approach	AAE	EPE	AAE	EPE
Average weight	2.514	0.170	3.919	0.518
Random	2.519	0.171	3.977	0.508
Closest	2.544	0.173	3.925	0.53
KLT	2.537	0.172	3.975	0.522

In order to show the relevance of our reliability score, Fig.6 display respectively the real errors AAE and EPE with respect to the reliability scores ranked in decreasing order (the value 0 corresponds to the highest reliability score), before and after propagation. First of all, the most reliable scores are actually related to a low error. Then, the propagation has reduced the errors magnitude in a significant way.

Final error measures for the height images are collected in Table.4. They are compared with the results provided by KLT (yves Bouguet, 2000), Horn and Schunk with $\lambda = 10$ (Horn and Schunck, 1981), Black and Anandan(BA) (Black and Anandan, 1996) that has the same form of energy function with Horn and Schunk but different error functions. In this case, BA uses the robust function Geman-McLure. We use the 8 sequences for which the ground truth is available on the MiddleBury website [4].

Experiments show that our method gives better results than the classic KLT or Horn and Schunck methods. Concerning the comparison with BA method, our method has greater performance on real scenes like ("RubberWhale","Hydrangea","Dimetrodon"). However, when using synthetic images ("Groove2","Groove3","Urban2","Urban3"), our approach still could be improved to distinguish better multiple flows that correspond to multiple motion in small regions, as visible in Fig. 7(c). Because the propagation is quite slow, with only 50 iterations, the reliable score is difficult to reach at every pixel. Hence, we can only correct the optical flow in a small region around the reliable motion. In some images, different false estimated motions in a large region can cause consequently a false reliable flow to be propagated as it is shown in Fig. 7(d) (the blue line). We can note that some of the problems that were mentioned before come from the inherent inaccuracy of KLT as it uses only intensity to estimate flow.

7 CONCLUSION

Starting from a classical optical flow method like KLT, we have proposed a new approach to improve optical flow precision by exploiting a flow reliability measure and a propagation strategy based on color and proximity. The advantage of this new strategy is to estimate the optical flow more precisely through propagation of reliable flows. Note that the idea could be extended to other optical flow techniques.

First results are promising as they show that our approach give better results than two classic methods (KLT and Horn and Schunk). The method is ranked 80/120 in the Middleburry evaluation

Moreover, our basic idea could be easily extended by considering other image features such as texture

[2]Average Angular Error

[3]End Point Error

[4]http://vision.middlebury.edu/flow/data/

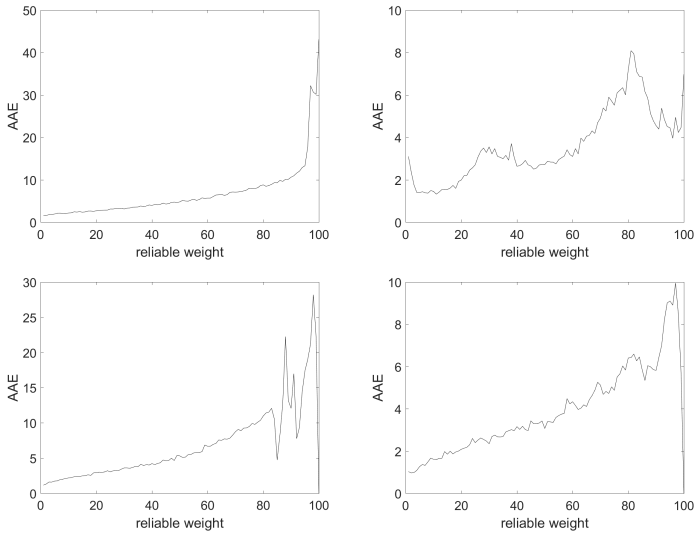

(a) (b)

Figure 6: Relation between reliable weight vs. AAE on two sequences (top: RubberWhale, bottom: Urban2): a) AAE before propagation b) AAE after propagation.

(a) (b) (c) (d)

Figure 7: Optical flow before (first line) and after propagation (second line).

Table 4: Performance of the compared methods in the Middlebury database.

Database	Venus		Dimetrodon		Hydrangea		RubberWhale		Groove2		Groove3		Urban2		Urban3	
Method	AAE	EPE	AAE	EPE	AAE	EPE	AAE	EPE	AAE	EPE	AAE	EPE	AAE	EPE	AAE	EPE
Proposed method	**4.054**	0.261	**3.877**	**0.194**	**2.422**	**0.221**	**3.558**	**0.114**	2.514	0.170	5.940	0.624	3.919	0.518	4.429	0.739
KLT	10.737	0.729	5.958	0.289	3.756	0.328	6.113	0.203	3.143	0.231	7.21	1.043	7.262	1.035	7.989	2.194
HnS	5.6	0.34	4.767	0.232	3.008	0.257	5.175	0.16	2.719	0.196	6.315	0.649	4.924	0.562	6.943	0.756
BA	4.095	**0.255**	4.199	0.205	2.665	0.231	4.384	0.132	**2.274**	**0.159**	**5.711**	**0.584**	**2.804**	**0.355**	**3.528**	**0.456**

or gradient and then by considering other reliability measures. Future work will consider other image features and try to reduce computational cost.

REFERENCES

Bab-Hadiashar, A. and Suter, D. (1998). Robust Optic Flow Computation. *International Journal of Computer Vision*, 29(1):59–77.

Baker, S., Scharstein, D., Lewis, J. P., Roth, S., Black, M. J., and Szeliski, R. (2010). A Database and Evaluation Methodology for Optical Flow. *International Journal of Computer Vision*, 92(1):1–31.

Black, M. J. and Anandan, P. (1991). Robust dynamic motion estimation over time. In , *IEEE Computer Society Conference on Computer Vision and Pattern Recognition, 1991. Proceedings CVPR '91*, pages 296–302.

Black, M. J. and Anandan, P. (1996). The Robust Estimation of Multiple Motions: Parametric and Piecewise-Smooth Flow Fields. *Computer Vision and Image Understanding*, 63(1):75–104.

Brox, T. and Malik, J. (2011). Large Displacement Optical Flow: Descriptor Matching in Variational Motion Estimation. *IEEE Transactions on Pattern Analysis and Machine Intelligence*, 33(3):500–513.

Brox, T. and Weickert, J. (2002). Nonlinear Matrix Diffusion for Optic Flow Estimation. In Gool, L. V., editor, *Pattern Recognition*, number 2449 in Lecture Notes in Computer Science, pages 446–453. Springer Berlin Heidelberg. DOI: 10.1007/3-540-45783-6_54.

Chen, Z., Jin, H., Lin, Z., Cohen, S., and Wu, Y. (2013). Large Displacement Optical Flow from Nearest Neighbor Fields. pages 2443–2450. IEEE.

Farneback, G. (2000). Fast and accurate motion estimation using orientation tensors and parametric motion models. volume 1, pages 135–139. IEEE Comput. Soc.

Horn, B. K. and Schunck, B. G. (1981). Determining optical flow. *Artificial Intelligence*, 17(1-3):185–203.

Kim, T. H., Lee, H. S., and Lee, K. M. (2013). Optical Flow via Locally Adaptive Fusion of Complementary Data Costs. pages 3344–3351. IEEE.

Liu, H., Chellappa, R., and Rosenfeld, A. (2003). Accurate dense optical flow estimation using adaptive structure tensors and a parametric model. *IEEE Transactions on Image Processing*, 12(10):1170–1180.

Lucas, B. D. and Kanade, T. (1981). An Iterative Image Registration Technique with an Application to Stereo Vision. pages 674–679.

Middendorf, M. and Nagel, H. H. (2001). Estimation and interpretation of discontinuities in optical flow fields. In *Eighth IEEE International Conference on Computer Vision, 2001. ICCV 2001. Proceedings*, volume 1, pages 178–183 vol.1.

Nagel, H.-H. and Gehrke, A. (1998). Spatiotemporally adaptive estimation and segmentation of OF-fields. In Burkhardt, H. and Neumann, B., editors, *Computer Vision — ECCV'98*, number 1407 in Lecture Notes in Computer Science, pages 86–102. Springer Berlin Heidelberg. DOI: 10.1007/BFb0054735.

Sun, D., Roth, S., and Black, M. J. (2010). Secrets of optical flow estimation and their principles. pages 2432–2439. IEEE.

Wedel, A., Pock, T., Zach, C., Bischof, H., and Cremers, D. (2009). An Improved Algorithm for TV-L 1 Optical Flow. In Hutchison, D., Kanade, T., Kittler, J., Kleinberg, J. M., Mattern, F., Mitchell, J. C., Naor, M., Nierstrasz, O., Pandu Rangan, C., Steffen, B., Sudan, M., Terzopoulos, D., Tygar, D., Vardi, M. Y., Weikum, G., Cremers, D., Rosenhahn, B., Yuille, A. L., and Schmidt, F. R., editors, *Statistical and Geometrical Approaches to Visual Motion Analysis*, volume 5604, pages 23–45. Springer Berlin Heidelberg, Berlin, Heidelberg.

Weinzaepfel, P., Revaud, J., Harchaoui, Z., and Schmid, C. (2013). DeepFlow: Large displacement optical flow with deep matching. In *IEEE Intenational Conference on Computer Vision (ICCV)*, Sydney, Australia.

Xu, L., Jia, J., and Matsushita, Y. (2010). Motion detail preserving optical flow estimation. pages 1293–1300. IEEE.

Yang, J. and Li, H. (2015). Dense, accurate optical flow estimation with piecewise parametric model. pages 1019–1027. IEEE.

yves Bouguet, J. (2000). Pyramidal implementation of the lucas kanade feature tracker. *Intel Corporation, Microprocessor Research Labs*.